Andrzej WAINDOK

Politechnika Opolska, Katedra Elektrotechniki Przemysłowej

A Method for Calculation of the Inrush Current in Single Phase Transformer including the Residual Flux

Streszczenie. *Przedstawiono polową-obwodową metodę obliczania przebiegów czasowych w dwuuzwojeniowym transformatorze jednofazowym. Przeanalizowano pole magnetyczne od prądów wzbudzenia oraz określono jego parametry całkowe. Uwzględniając parametry schematu zastępczego oraz magnetyczny strumień remanentu w rdzeniu ze stali krzemowej, wykorzystano opracowaną metodę do analizy stanów nieustalonych, w szczególności załączania transformatora. Jako przykład numeryczny obliczono przebieg prądu załączania dla uzwojenia wewnętrznego oraz zewnętrznego. Obliczone krzywe prądu porównano z wynikami pomiarów dla transformatora1-fazowego* ***(Metoda obliczania prądu załączania transformatora jednofazowego z uwzględnieniem strumienia remanentu)***

Abstract*. A field-circuit method for simulation of transients in a single-phase, two-winding transformer has been given. The magnetic field excited by the winding currents has been analyzed, and integral parameters have been determined. Including the equivalent circuit parameters and the magnetic residual flux in the silicon steel core, the developed method has been implemented for the transitional states, especially for the transformer switching on. As numerical examples, the waves of the inrush current have been calculated in terms of the internal winding as well as external one supplying. Calculated waves of the inrush current were compared with those obtained experimentally from the tests of the single-phase transformer.*

Słowa kluczowe: obliczenia pola magnetostatycznego, metoda polowo-obwodowa, prąd załączania, strumień remanentu, transformatory.
Keywords: magnetostatic field analysis, field–circuit method, inrush current, residual flux, transformers.

Introduction

When a transformer is taken off- line, there will be amount of the so called residual magnetic flux, which remains in the core due to the properties of the magnetic material. Depending on the core steel, the residual flux can be up to 80% of the operating main flux [1]. When the supplying voltage is reapplied to the transformer, the magnetic flux excited by the source voltage will be build upon that which already exists in the core. In order to maintain this level of the flux in the core, which can be in saturation range of the core steel, the transformer can draw current well in excess of the transformer's rated load current. Depending on the transformer design, the magnitude of the inrush current can be from 3.5 to 40 times greater than the rated current [1].

In computer aided designing (CAD) of transformers, not only the steady-state parameters are important, but also the transitional ones should be taken into account. Especially, the current waves upon when the transformer is switching on, are very important for designing of the insurance relays. The inrush currents can have an effect on the transformer operation and on the relays and fuses located in the power system where the transformer operates. The benefits of our computer simulations and the current determination are well recognized. Knowledge of their values is also important for correct determination of the parameters in the shelters [2].

Decent approximations of the inrush current require detailed information regarding the transformer parameters [1]. When its physical model is approachable, the equivalent circuit parameters can be simply obtained from measurements. However, during the transformer designing, they can be obtained only from computer simulations e.g. from magnetic field calculations [3, 4, 5, 6, 7, 8].

The transients of transformers were analyzed in many works e.g. [9, 10, 11, 12]. In some of them, the hysteresis effects were also taken into account [10, 12]. However, there are not many researches, where the residual (remanent) flux was considered for the transformer soft magnetic material. In this work we carried out the calculations using the equivalent circuit parameters, and including different values of the remanent flux. We have simulated the single-phase transformer operation and its transient states. Using magnetic field analysis, the non-linear characteristic of the magnetizing inductance, as a function of magnetizing current, was determined and the leakage inductances were computed. In the computations the material characteristics were included and the magnetic remanent has been indirectly taken into account as an initial value of the magnetizing current. We have studied the inrush current waves in terms the internal and external (to the transformer legs) winding excitation, as well.

The transformer to be investigated as a numerical example

The measurement verification of the field-circuit method has been done for a single-phase transformer, produced in Poland (Fig. 1). This type of transformer is used for medical equipment, and incorporates design features in both the insulation and values of the current transient that allow be tailored to meet operational and safety requirements [2]. Hence, low inrush currents are forced to be as low as possible [2]. Obviously, they depends on the electromagnetic system of transformer, and the moment of turning it on and off.

To overcome the inconvenient moments of plugging the transformer (in power system) some electronic switches can be employed. The starting currents are considerably higher than the operating ones, and the overall cost of the power electronic controller is high. Thus, even for small transformers, it is an expensive venture from economic point of view.

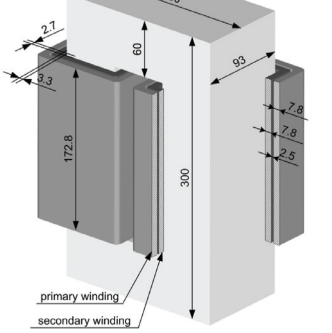

Fig. 1. Coil and core dimensions of the tested transformer

The dimensions of the coils and magnetic core of the investigated transformer are given in Fig. 1. It is a single-phase core-form construction. The nominal supplying voltage and current, (at the frequency of 50 Hz) are U_N=230 V and I_N=22.5 A, respectively. Its nominal power is relatively low, S_N=5 kVA. Number of turns of the primary winding (external one, Fig. 1) is N_1=182. As the voltage ratio is nearly equal to unity, the turn number of the secondary winding (internal one) is N_2=188. Primary and secondary windings are halved and located on both core legs. They were wound using the same bus wire of 2.5 mm x 4 mm cross-section.

We have done many calculations and tests, but due to brevity, we present the calculation and experimental results for one variant (case) of the transformer electromagnetic system. We assumed that the value of the input voltage (U_{1N}) is the power line one (U_N=230 V). One may add that the short circuit voltage of the investigated transformer is $U_{z\%}$=2.57% and the value of the steady-state no-load current is $I_{0\%}$=0.79%.

Formulation of the magnetic field equations

In thin winding wires (with small cross-section) as well as in very thin ferromagnetic sheets, the eddy currents are very low and their influence on the core magnetic flux and winding inductances is not significant. As the transformer cores are stacked with thin laminated silicon steel sheets, we have neglected in our calculation model the eddy currents influence on the main magnetic flux [3, 5, 13].

In the magnetic field simulations, the material characteristics have to be included. Each designer usually employs the B/H curve and the total losses in the core for the core material e.g. silicon steel sheets. The curve can be available from a producer as a function of magnetic intensity [1]. We included the nonlinear B/H curve of the silicon steel M111-35N (Fig. 2).

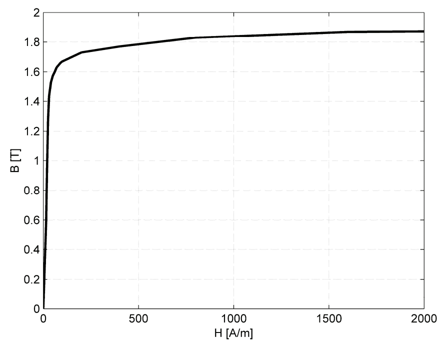

Fig. 2. B/H curve of the grain-oriented silicon steel M111-35N

For the magnetic field analysis scalar potential formulation has been performed. Two potentials have been introduced in the non-linear partial differential equations (PDE), which govern various subregions. In the areas with the excitation currents, the reduced scalar potential ϕ is employed, which is expressed by the PDE [14]:

(1a) $$\nabla \cdot (\mu \nabla \phi) - \nabla \cdot \mu \vec{H}_s = 0$$

where $\vec{H}_s$ - the field produced by all of the excitation currents.

For other subregions e.g. iron regions (magnetic core) the total scalar potential ψ is introduced

(1b) $$\nabla \cdot (\mu \nabla \psi) = 0$$

As the subregions of the transformer field area are nonhomogenous, we must join the potentials ϕ and ψ at the interregion boundaries. Including the interface conditions, there is possibility to remove the discontinuity (of the two potentials) at the interface Γ_{ie} between the two regions (Ω_i and Ω_e). The normal components of the magnetic flux density and the tangential components of the field intensity must be equal each other both sides of the interface. When the unit vectors $\vec{n}_i$ and $\vec{t}$ are normal and tangential vectors to the interface Γ_{ie}, the interface conditions can be rewritten as

(2) $$\mu_i(-\nabla\psi) \cdot \vec{n}_i = \mu_e(\vec{H}_s - \nabla\phi) \cdot \vec{n}_i$$

(3) $$-(\nabla\psi) \cdot \vec{t} = (\vec{H}_s - \nabla\phi) \cdot \vec{t}$$

For the transformer magnetic field analysis the Dirichlet's conditions ϕ=0 and ψ=0 have been assumed at the boundaries of the calculated regions. One should add, that it is due to the construction without ferromagnetic casing. The Neumann's conditions dϕ/dn=0 and dψ/dn=0 have been established at the symmetry plane of the calculated region. Symmetry conditions were exploited to reduce the problem domain to a quarter of the transformer.

The finite element package has been used for the field simulation. For the current carrying regions i.e. windings, the reduced scalar potential ϕ was introduced. For the regions without current, we can introduce the total scalar potential ψ. Considering the symmetry conditions we obtained the finite element mesh with 75000 first-order elements. Particular care was taken for appropriate discretization in the vicinity of the air gaps and the core surface as well as their edges.

The magnetic flux path in the iron region of the no-loaded transformer is largely collinear to the plane of the core laminations, and hence the substitute air-gaps in the joins of the sheets in the laminated core have been established. For no-load state of transformer, the characteristic of the main flux in magnetic circuit vs. the magnetizing current can be determined from the field analysis and included to the equivalent circuit which has been developed in this work.

No-load state

We have calculated flux density values in many subregions of the transformer core for the no-load state. However, due to brevity we present only the distributions (histograms), (Figs. 3 and 4) concern the surface (z=2 cm) situated above the plane of symmetry (z=0, Fig. 3a). They have been obtained for the rms current value I_0=0.178 A in the excited winding, which is respondent to the nominal supply voltage.

For the no-load state of the analyzed transformer almost all magnetic flux is squeezed inside the ferromagnetic material of the core (Fig. 3b). Field intensity values depend on the location of the supplied winding respect to the core leg, which is shown in Figs. 3c and 3d. They are lower in the case when the internal winding is supplied (Fig. 3d). If the external winding is excited under the same current, the values of the magnetic field intensity are about 2 times greater (Fig. 3c) than those depicted in Fig. 3d. From Fig. 3, we can see that under the no-load state, the maximum values of the magnetic flux density not exceed 1.12 T, for the rated voltage.

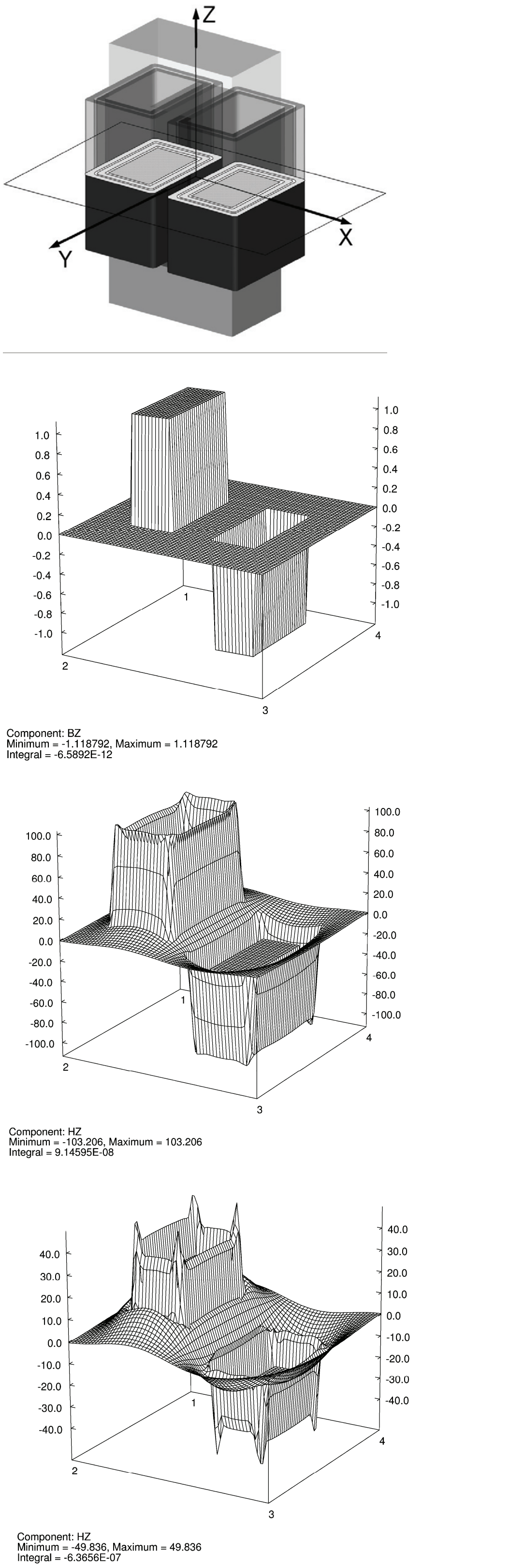

Fig. 3. Histograms of the B (in Tesla) and H (in A/m)values at the points of the plane z=2 cm for no-loaded transformer (a) in the XY cross section: (b) B_Z component, (c) H_Z component for external winding excitation, (d) H_Z component for internal winding excitation.

Short circuit state

The short-circuit state has also been studied for obtaining the leakage reactances of the windings [4, 13]. We have calculated the field values for the rated currents of the transformer shown in Fig. 1. We assumed the balance of the amperturns $I_1N_1 = I_2N_2 = 4095$ A. Under shorting of the transformer winding the magnetic field arises inside the aircanals (airgaps). It is in the interregions between the external and internal coaxial windings. Due to the outer field analysis, the external boundaries of the calculated region were established much farther from the core surface than the boundaries assumed for the no-load state.

The magnetic flux density distribution, for the short-circuit state, is presented in Fig. 4a. Under this state, the flux lines concentration is visible in the area between primary and secondary windings. Due to unbalanced field intensities excited by the windings, slight values of the magnetic flux density in the cross-sections of the transformer legs are depicted in Fig. 4a. The flux density values in the region don't exceed 0.015T.

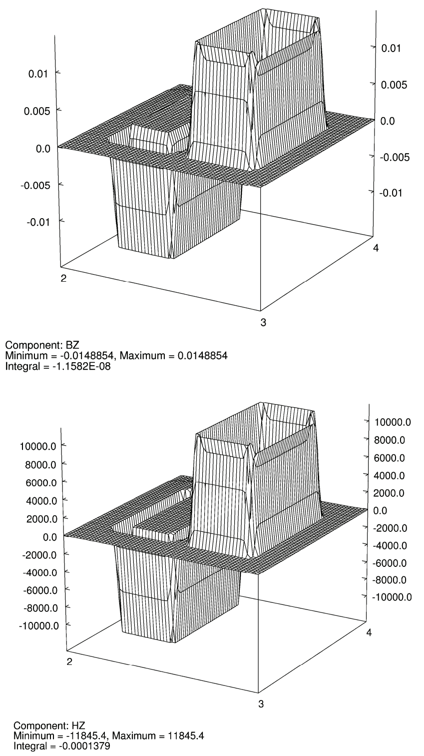

Fig. 4. Histograms for the transformer (presented in Fig. 1) under short-circuit: (a) B_Z component [T], (b) H_Z component [A/m]

Transformer parameters determination

The equivalent circuit of a transformer consists of winding resistances (R_1, R_2), leakage inductances of the windings (L_{s1}, L_{s2}), core loss resistance R_{Fe} and the magnetizing inductance L_μ [1]. The last-mentioned quantity changes according to the voltage and current variations, and is mostly given as a non-linear characteristic vs. current values.

Considering the winding and wire dimensions, we could easily calculate the winding resistances of the transformer (Fig. 1). For primary and secondary windings the values are: R_1=0.136 Ω and R_2=0.114 Ω.

The magnetizing inductance of the transformer was obtained from magnetic flux linkage values. This method has been developed and employed by the author of this work. It is precise enough [4, 13]. The flux linkage Ψ can be found as a sum of the magnetic fluxes Φ_k. Each of them is linked with k^{th} turn

(4) $$\Psi = \sum_{k=1}^{N} \Phi_k$$

For the relative thin winding wire the flux Φ_k is obtained after integration of the magnetic flux density (B) distribution over the surface resting on the geometrical axis of the k^{th} wire.

Knowing the flux linkage under the current I excitation we obtained the magnetizing inductance L_μ

(5) $$L_\mu = \frac{\Psi}{I}$$

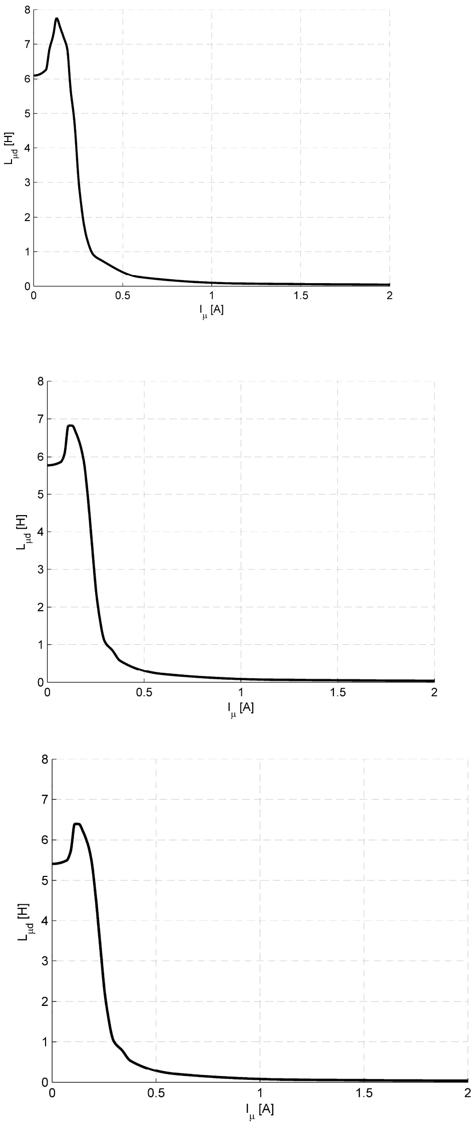

Fig. 5. Dynamic inductance vs. the magnetizing current: (a) primary winding excitation (N_1=182), (b) secondary winding excitation (N_2=188), (c) simulated inductance for virtual secondary winding with N_2^*=182.

As the magnetizing inductance L_μ strongly depends on the magnetizing current, it is impossible to obtain experimentally its values for full range of the current intensity. However, we can simulate the L_μ function after calculating the integral parameter for different values of the exciting current. The simulation results were used for obtaining the characteristic of the so-called dynamic inductance $L_{\mu d}$ as a function of the magnetizing current (Fig. 5).

(6) $$L_{\mu d} = \frac{d\Psi}{di_\mu}$$

When the turn number is increasing, the inductance value is going up. However, form Fig. 5b it is visible that the inductance (for N=188) is lower than that linked with N=182 turns. It is due to the fact that the derivative (6) depends on the winding location in relation to the core leg.

Figures 5a and 5c illustrate the $L_{\mu d}$ graphs for the external and internal (to the core leg) windings having the same turn numbers. For the external winding, the uppermost value of the inductance (Fig. 5a) is about 20% higher than that for the internal one (Fig. 5c). If the turn number is increasing by 3% referring the tested transformer winding, the inductance increases by 6.5%. We also observed some little saddles in the initial fragments of $L_{\mu d}$ graphs. They are due to precisely including the initial pieces of the silicon steel B/H curve.

One should underline that transformer designers include only one value of the magnetizing inductance, which does not allow correct determination the inrush current.

The magnetic field analysis under short-circuit state was carried out, to obtain the transformer leakage inductances [3, 5]. We realize the difference between L_{s1} and L_{s2} values. However, for the transient analysis [1, 3] the discrepancy is not significant. Thus, we assumed the values to be equal. After calculating the energy of magnetic field W we have used the known formula:

(7) $$L_{s1} = L_{s2} = \frac{1}{2}\frac{2 \cdot W}{I^2} = \frac{W}{I^2}$$

where: I – rms value of the excitation current.

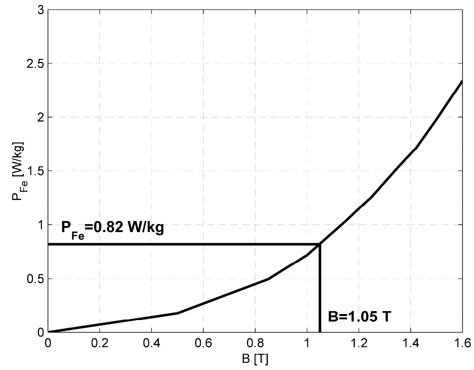

Fig. 6. Core losses per kilo of the iron

Involving the magnetic energy W=89.64·10^{-3} J, and the rated current I_1=I_2=22.5A values, we calculated the leakage inductances L_{s1}=L_{s2}=177μH.

The sheets from silicon, grade oriented steel almost always have been stacked into the magnetic cores. The laminated sheets limit the iron losses. Thus, the hysteresis loop can be included indirectly by taking into consideration the magnetic remanent B_{res} and core loss resistance R_{Fe} values. To obtain the R_{Fe} value, we employed the core losses characteristic (Fig. 6). Due to low flux density under the transformer operation (approximately 1T), the core losses are relatively low. Including the transformer core mass (m=29.5 kg) and the operation flux density, we obtained the loss resistance value R_{Fe}=2186 Ω.

The equivalent Γ-circuit (Fig. 7) was used for simulation the non-load state of the transformer. To calculate the magnetization current, we had to included the magnetic remanent B_{res} value in the core cross-section. The equivalent circuit parameters obtained from the calculations and tests are compared in table 1. One ought to emphasize that the leakage reactance value obtained from the field analysis is close to the measured one. The discrepancy between measured and calculated values of the R_{Fe}, is not significant for the calculation of the transient currents.

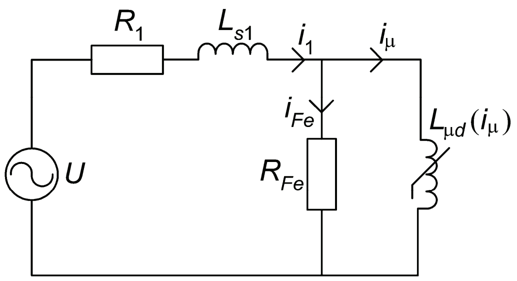

Fig. 7. Equivalent circuit of a transformer for no-load state

Table 1. Parameters of the transformer diagram

Parameter	Calculated	Measured
L_{s1} [μH]	177	174
R_1 [mΩ]	136	132
R_2 [mΩ]	114	114
R_{Fe} [Ω]	2186	2405

Time simulations of the transformer transients

The field-circuit method was employed to studying the transformer transients. The circuit equations were obtained using Lagrange'a method [15]. The source (excitation) current i_1 and magnetizing current i_μ were chosen as generalized quantities. The following system of equations is expressed as:

$$\begin{cases} L_{s1}\dfrac{di_1}{dt} = u - R\cdot i_1 + R_{Fe}\cdot(i_\mu - i_1) \\ L_{\mu d}(i_\mu)\dfrac{di_\mu}{dt} = -R_{Fe}\cdot(i_\mu - i_1) \end{cases} \tag{8}$$

From the equations above, time derivative of the magnetizing current can be obtained:

$$\frac{di_\mu}{dt} = \frac{-R_{Fe}\cdot(i_\mu - i_1)}{L_{\mu d}(i_\mu)} \tag{9}$$

In our algorithm, the magnetizing current has been calculated from the integral given below:

$$i_\mu = \int \frac{-R_{Fe}\cdot(i_\mu - i_1)}{L_{\mu d}(i_\mu)}dt + i_\mu(0) \tag{10}$$

The initial value $i_\mu(0)$ strongly depends on the residual flux density B_{res}. Taking into account the operation flux and the residual flux density, the magnetic permeability values were calculated. For a single phase transformer, with ferromagnetic core, the $i_\mu(0)$ value can be estimated from the transformer electromagnetic system with the equation

$$i_\mu(0) = \frac{B_{res}\cdot l}{\mu(H)\cdot N} \tag{11}$$

where: l – average length of the magnetic flux lines, $\mu(H)$ - nonlinear magnetic permeability, N – number of winding turns.

In computer simulations, we can determine the $L_{\mu d}$ as a function of the different values of the current intensity. The function $L_{\mu d}(I)$ has been implemented using the "look-up table" module given in the "nonlinear block" of the algorithm.

The simulation of inrush-current at a no-load transformer can introduce some difficulties in the calculation process, because the resulting system of equations is numerically ill conditioned. In the nonlinear circuit, the tightly-coupled windings, with relatively small value of the leakage inductance, cause the numerical errors. To avoid the numerical instability, we had to pick an integration method, which was suitable for stiff systems. In our problem, we have used Gear's backward difference formula (BDF) [16]. It is excellent for solving stiff systems with eigenvalues not close to the imaginary axis.

Inrush current calculation for the primary winding excitation

Fig. 8 shows the calculated current waves for three values of the residual flux density B_{res}. The values of the wave envelope, obtained with assumption B_{res}=0.8 T and B_{res}=1.2 T amount to hundreds of ampers. We can observe that the residual magnetism has strong effect on the inrush current. The current values are about one hundred times greater than those simulated without the residual magnetism.

During the measurements there is no information about the residual flux density B_{res} value (it is a stochastic quantity). Thus, the measured waves (Fig. 9) differ from the calculated ones. We realized that under the tests the commutation moment is not very precisely determined.

It is observed a fine attenuation of the current waves (Fig. 8). It seems, that in the measured case under the transformer switching on, the B_{res} value approximates 1.2 T. The computation and measurement values of the current peaks for the B_{res} value 1.2 T are given in table 2.

Table 2. Simulated and Measured Current Peaks for B_{res}=1.2 T (Fig. 8c)

Peak number	1	2	3	4	5
Calculated	313	209	152	116	92
Measured	320	112	60	44	-

Secondary winding excitation

The inrush current wave depends on the winding (of the transformer) to be plugging in, naturally. If we apply the voltage to the primary (N_1=182) winding, we obtain the waves presented in Figs. 8 and 9. Figures 10 and 11 relate the secondary (N_2=188) one supplying. Calculations, as well as measurements show that the current peak I_{0max} is greater than that obtained for the primary (outer) winding supplying. The first reason is that the secondary winding is placed near the core, so the resistance is lower than those for the primary one. The second one, most significant, is that the characteristic $L_{\mu d}=f(i_\mu)$ is lower for the winding, which is closer to the core leg. From Fig. 5 it is visible, that a small modification of the $L_{\mu d}=f(i_\mu)$ curve causes significant variation in the inrush current wave.

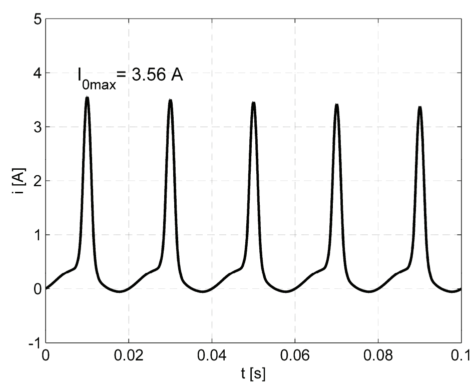

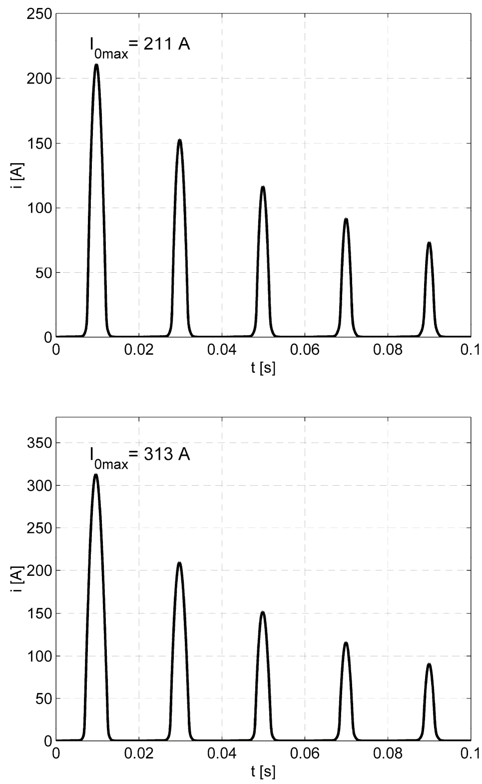

Fig. 8. Current waves for primary winding: (a) without remanence (B_{res}=0), (b) B_{res} = 0.8 T, (c) B_{res} = 1.2 T.

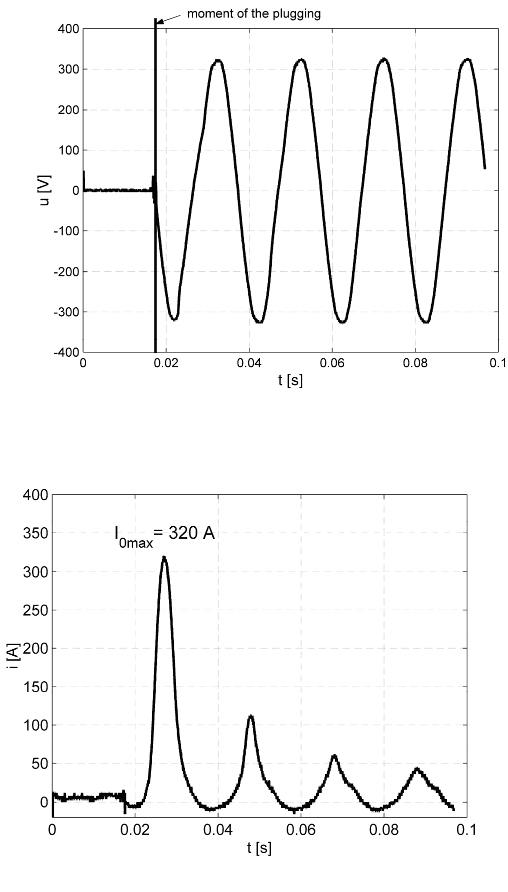

Fig. 9. Measured waves for switching on the primary winding: (a) voltage, (b) current.

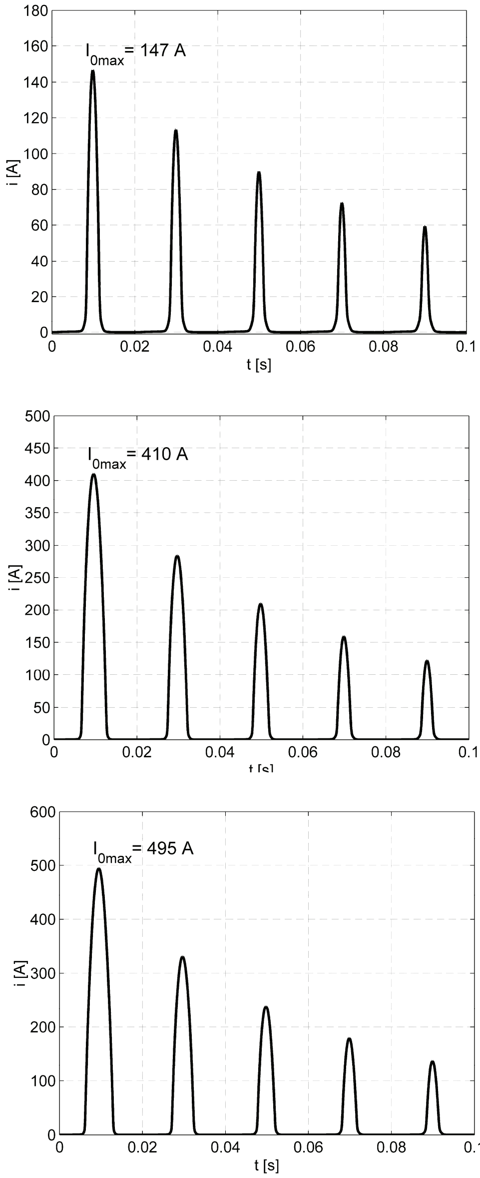

Fig. 10. Current waves for secondary winding (N_2=188) excitation: (a) B_{res}=0, (b) B_{res} = 0.8 T, (c) B_{res} = 1.2 T

The dropping of the current wave envelope is more intensive for experiment (Fig. 11, table 3). The first current peak, calculated for the B_{res}=1.2 T, considerably exceeds the measured value (Fig. 10c). It is partially due to the residual flux value, which has been assumed for the simulation.

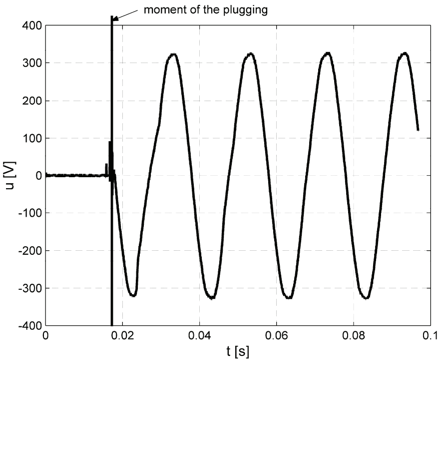

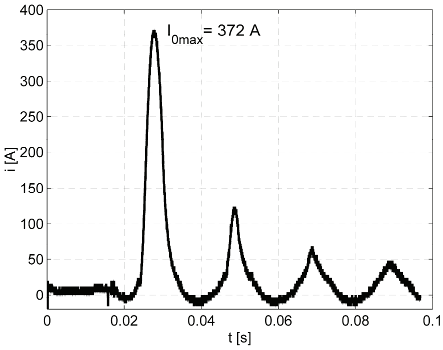

Fig. 11. Measured waves under switching on the secondary winding: (a) voltage, (b) current

Table 3. Simulated and Measured Current Peaks for B_{res}=1.2 T (Fig. 10c)

Peak number	1	2	3	4	5
Calculated	495	330	238	179	137
Measured	372	124	68	48	-

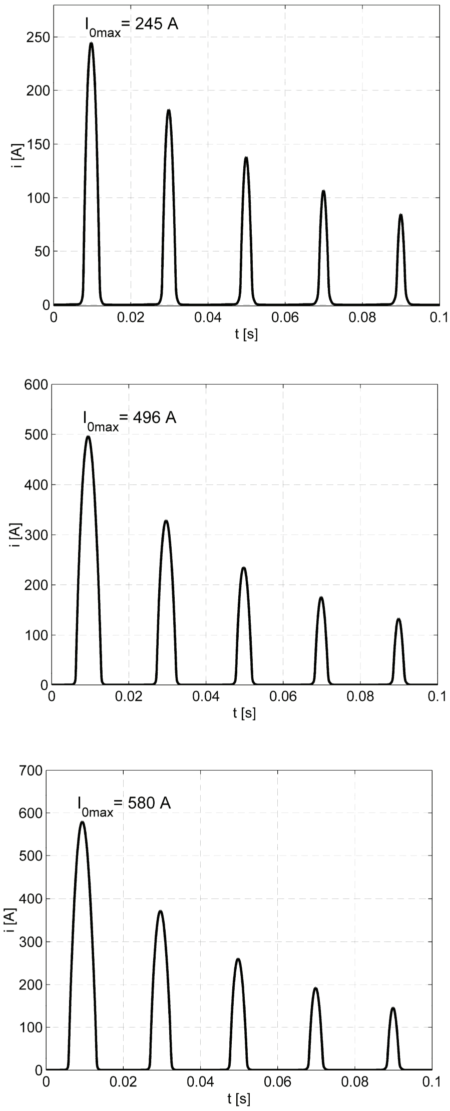

Fig. 12. Current waves for the secondary winding excitation (N_2^*=182): (a) B_{res}=0, (b) B_{res} = 0.8 T, (c) B_{res} = 1.2 T

To show the influence of the turn number of the primary winding, we calculated the inrush current in the virtual transformer with the same geometry as the tested one, but for the same number of turns (N_1=182, N_2=182). The first current peak is greater in the case. It is from 17% to 67% greater (Fig. 12) than those for N_2=188, depending on B_{res} value. The current wave attenuation does not change significantly.

Comparison of the calculated waves under supplying either primary or secondary windings

In this paper we have shown that the inrush current values depend on the side which is supplied, even for the transformer with the voltage ratio which is equal to unity. We calculated and measured the inrush currents for excitation of primary and secondary windings, as well.

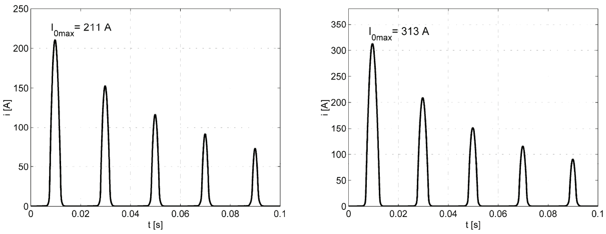

Primary (external) winding excitation (N_1=182)

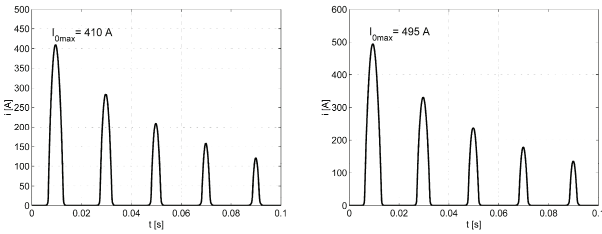

Secondary (internal) winding excitation (N_2=188)

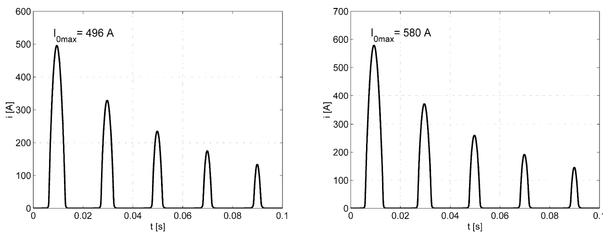

Secondary (internal) winding excitation (N_2^*=182)

Fig. 13. Comparison between primary and secondary winding current: (a) B_{res} = 0.8 T, (b) B_{res} = 1.2 T

Comparison between I_{0max} values obtained from calculations for the primary winding excitation and the secondary one, is shown in Fig. 13. Assuming the same turn number of the windings (N_2=182), we observed the differences in the current waves. They mainly depend on the residual flux density B_{res} value. Comparing both cases, one ought to emphasize, that the greater value of the inrush current occurs for the internal winding excitation, naturally. The current value is about 85-135% higher, than that for external winding excitation. It is due to lower dynamic inductance and lower resistance for internal winding. For the N_2=188 turns in the internal winding the first peak of inrush current is about 14-17% lower than that for N_2=182, depending on the B_{res} value.

Conclusions

Our simplified method, with the residual magnetic flux including, is helpful for prediction the maximum values of the inrush current waves. The field-circuit model for simulation of transformer transients has been used to calculate the inrush current waves. The equivalent circuit parameters were determined using numerical methods, such as the FEM in the field analysis.

It is well known, that the inrush current depends on the core magnetization history, especially the hysteresis loop and the moment of the transformer plugging. For simplifying the field-circuit calculations we included the magnetic flux density remanence B_{res} into our mathematical model. The residual flux significantly affects the inrush current wave.

The field calculations make visible differences between the current waves for two designs of the medical transformer. The first design relates to the outer- and the second to the inner coils as the primary winding. The tested transformer nominal operation establishes the outer ones as the primary winding.

For supplying of the winding situated near the core, the I_{0max} value is greater than that for the nominal conditions. The attenuation of the current wave is less significant in the case, as well. Thus, as we need to limit the I_{0max} value, we have to fix the primary winding on the secondary one, which is closer to the core column than the secondary one.

The calculation method presented in this work is validated by measurements for the single-phase transformer. We observed relatively good conformity between computed and measured current waves. The differences between calculation and measurement results arise from the field analysis and measurement errors. For example, the residual flux, included by the B_{res} value, is difficult to determine by some measurements, and contributes to the errors of our method, as well.

Praca współfinansowana przez MNiSW w ramach projektu własnego nr N N510 533739.

LITERATURA

[1] Grigsby L. L., The Electric Power Engineering Handbook, CRC Press LLC, 2001.
[2] IEC 61558-2-15: Safety of power transformers, power supply units and similar – Part 2-15: Particular requirements for isolating transformers for the supply of medical locations, 1999-02.
[3] Tomczuk B., Analysis of 3-D magnetic fields in high leakage reactance transformers, *IEEE Trans. on Magn.*, 30 (1994), no.5, 2734-2738.
[4] Tomczuk B., Three-Dimensional Leakage Reactance Calculation and Magnetic Field Analysis for Unbounded Problems, *IEEE Trans. on Magn.*, 28 (1992), no.4, 1935-1940.
[5] Tomczuk B., Babczyk K., Calculation of the Self- and Mutual Inductances and 3-D Magnetic Fields of Chokes with Air Gaps in the Core, *Electrical Engineering,* Springer, 2001, no. 83, 41-46.
[6] Zakrzewski K., Tomczuk B., 3-D Magnetic Field Distribution of Yoke Flux in Three-Phase Transformers without Ferromagnetic Tanks, *COMPEL- The International Journal for Computation and Mathematics in Electrical and Electronic Engineering*, 13 (1994), no.1, 93-96.
[7] Zakrzewski K., Tomczuk B., Magnetic Field Analysis and Leakage Inductance Calculations in Current Transformers by Means of 3-D Integral Methods, *IEEE Trans. on Magn.*, 32 (1996), no.3, 1637-1640.
[8] Tomczuk B., Metody numeryczne w analizie pola układów transformatorowych, Oficyna Wydawnicza Politechniki Opolskiej, Opole, 2007.
[9] Koppikar D. A., Kulkarni S. V., Khaparde S. A., Arora B., A modified approach to overfluxing analysis of transformers, *Electrical Power & Energy Systems*, 20 (1998), no.4, 235-239.
[10] Salerno C. H., Bispo D., Camacho J. R., Neto L. M., A non-linear analysis of a single-phase transformer, *ICEM'02,* Brugge, Belgium, 26-28 September 2002, 303-309.
[11] Tomczuk B., Koteras D., Zimon J., Waindok A., Calculation of the transient currents in transformers using field-circuits methods, *Przegląd Elektrotechniczny (Electrical Review)*, 87 (2011), no. 11, 126-130.
[12] Wang X., Thomas D.W.P., Summer M., Paul J., Cabral S.H.L., Characteristics of Jiles-Atherton model parameters and their application to transformer inrush current simulation, *IEEE Trans. on Magn.*, 44 (2008), no. 3, 340-345.
[13] Tomczuk B., Zakrzewski K., Koteras D., Magnetic field and short-circuit reactance calculation of the 3-phase transformer with symmetrical amorphous core, in book *Computer Engineering in Applied Electromagnetism*, Springer, 2005, 227-230.
[14] Tomczuk B., Koteras D., Waindok A., Zimon J., Polowa analiza siłowników elektromagnetycznych i transformatorów, *Pomiary Automatyka Kontrola (PAK)*, 2011, no. 3, 264-268.
[15] Nasar S. A., Electromagnetic energy conversion*, Devices and Systems*, Prentice Hall Inc. Englewood Cliffs, 1980.
[16] Gear C. W., Numerical initial value problems in ordinary differential equations, Prentice Hall Inc., New Jersey, 1971.

***Autor**: dr inż. Andrzej Waindok, Politechnika Opolska, Instytut Układów Elektromechanicznych i Elektroniki Przemysłowej, Katedra Elektrotechniki Przemysłowej, ul. Prószkowska 76, 45-758 Opole, E-mail: a.waindok@po.opole.pl.*